Active Damping of Rotating Platforms using Integral Force Feedback

ISMA-USD 2020, September 7-9, 2020

Thomas Dehaeze [1,3]   Christophe Collette [1,2]

[1]Precision Mechatronics Laboratory, University of Liege, Belgium

[2]BEAMS Department, Free University of Brussels, Belgium

[3]European Synchrotron Radiation Facility, Grenoble, France

ESRF
The European Synchrotron

ISMA-USD
International Conferences on
Noise and Vibration Engineering
Uncertainty in Structural Dynamics

Outline

Outline

Model of a Rotating Positioning Platform

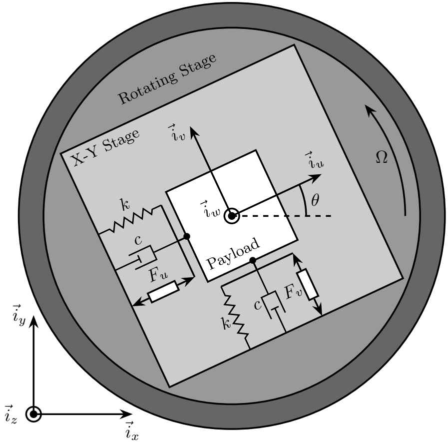

Fig.: Schematic of the studied System

Simplest model to study the **gyroscopic effects** on Decentralized IFF

Assumptions:

- Perfect Rotating Stage
- $\dot{\theta}(t) = \Omega = \text{cst}$
- Small displacements
- Position of the mass described by $[d_u \ d_v]$

Two frames:

- Inertial frame $(\vec{i}_x, \vec{i}_y, \vec{i}_z)$
- Uniform rotating frame $(\vec{i}_u, \vec{i}_v, \vec{i}_w)$

Equations of Motion - Lagrangian Formalism

$$\frac{d}{dt}\left(\frac{\partial L}{\partial \dot{q}_i}\right) + \frac{\partial D}{\partial \dot{q}_i} - \frac{\partial L}{\partial q_i} = Q_i$$

with $L = T - V$ the Lagrangian, D the dissipation function, and Q_i the generalized force associated with the generalized variable.

$$T = \frac{1}{2}m\left(\left(\dot{d}_u - \Omega d_v\right)^2 + \left(\dot{d}_v + \Omega d_u\right)^2\right), \quad V = \frac{1}{2}k\left({d_u}^2 + {d_v}^2\right)$$

$$D = \frac{1}{2}c\left({\dot{d}_u}^2 + {\dot{d}_v}^2\right), \quad Q_1 = F_u, \quad Q_2 = F_v$$

$$\begin{aligned} m\ddot{d}_u + c\dot{d}_u + (k - m\Omega^2)d_u &= F_u + 2m\Omega\dot{d}_v \\ m\ddot{d}_v + c\dot{d}_v + (k \underbrace{- m\Omega^2}_{\text{Centrif.}})d_v &= F_v \underbrace{- 2m\Omega\dot{d}_u}_{\text{Coriolis}} \end{aligned}$$

Centrifugal forces $\Longleftrightarrow$ Negative Stiffness
Coriolis Forces $\Longleftrightarrow$ Coupling

Transfer Function Matrix the Laplace domain

$$\begin{bmatrix} d_u \\ d_v \end{bmatrix} = \boldsymbol{G}_d \begin{bmatrix} F_u \\ F_v \end{bmatrix}$$

$$\boldsymbol{G}_d = \frac{1}{k} \begin{bmatrix} \frac{\frac{s^2}{{\omega_0}^2} + 2\xi\frac{s}{\omega_0} + 1 - \frac{\Omega^2}{{\omega_0}^2}}{\left(\frac{s^2}{{\omega_0}^2} + 2\xi\frac{s}{\omega_0} + 1 - \frac{\Omega^2}{{\omega_0}^2}\right)^2 + \left(2\frac{\Omega}{\omega_0}\frac{s}{\omega_0}\right)^2} & \frac{2\frac{\Omega}{\omega_0}\frac{s}{\omega_0}}{\left(\frac{s^2}{{\omega_0}^2} + 2\xi\frac{s}{\omega_0} + 1 - \frac{\Omega^2}{{\omega_0}^2}\right)^2 + \left(2\frac{\Omega}{\omega_0}\frac{s}{\omega_0}\right)^2} \\ \frac{-2\frac{\Omega}{\omega_0}\frac{s}{\omega_0}}{\left(\frac{s^2}{{\omega_0}^2} + 2\xi\frac{s}{\omega_0} + 1 - \frac{\Omega^2}{{\omega_0}^2}\right)^2 + \left(2\frac{\Omega}{\omega_0}\frac{s}{\omega_0}\right)^2} & \frac{\frac{s^2}{{\omega_0}^2} + 2\xi\frac{s}{\omega_0} + 1 - \frac{\Omega^2}{{\omega_0}^2}}{\left(\frac{s^2}{{\omega_0}^2} + 2\xi\frac{s}{\omega_0} + 1 - \frac{\Omega^2}{{\omega_0}^2}\right)^2 + \left(2\frac{\Omega}{\omega_0}\frac{s}{\omega_0}\right)^2} \end{bmatrix}$$

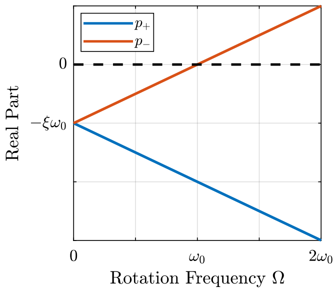

(a) Real Part

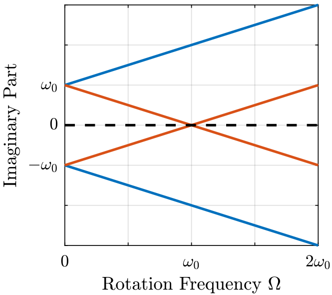

(b) Imaginary Part

Fig.: Campbell Diagram : Evolution of the complex and real parts of the system's poles as a function of the rotational speed Ω

Bode Plots of the System's Dynamics

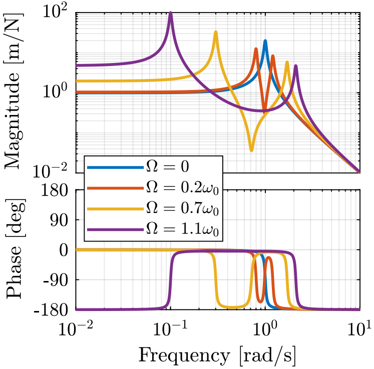

(a) Direct Terms d_u/F_u, d_v/F_v

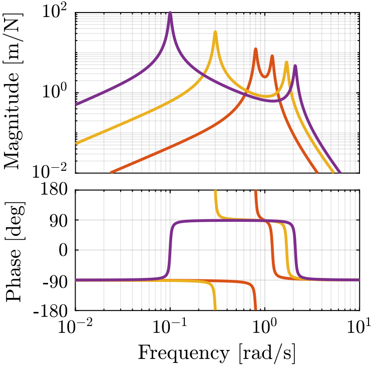

(b) Coupling Terms d_v/F_u, $-d_u/F_v$

Fig.: Bode Plots for $\boldsymbol{G}_d$ for several rotational speed Ω

For all the numerical analysis, $\omega_0 = 1\,\mathrm{rad\,s^{-1}}$, $k = 1\,\mathrm{N\,m^{-1}}$ and $\xi = 0.025 = 2.5\,\%$.

Outline

Force Sensors and Control Architecture

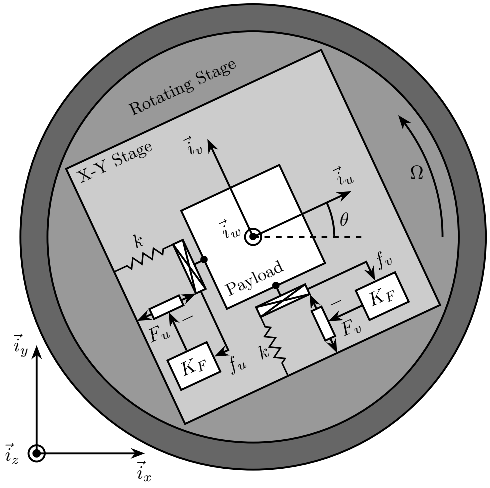

Fig.: System with added Force Sensor in series with the actuators

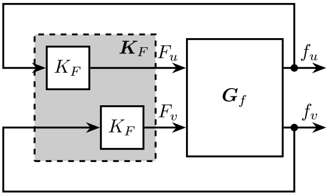

Fig.: Control Diagram for decentralized IFF

$$\boldsymbol{K}_F(s) = \begin{bmatrix} K_F(s) & 0 \\ 0 & K_F(s) \end{bmatrix}$$

$$K_F(s) = g \cdot \frac{1}{s}$$

Plant Dynamics

$$\begin{bmatrix} f_u \\ f_v \end{bmatrix} = \begin{bmatrix} F_u \\ F_v \end{bmatrix} - (cs + k) \begin{bmatrix} d_u \\ d_v \end{bmatrix}$$

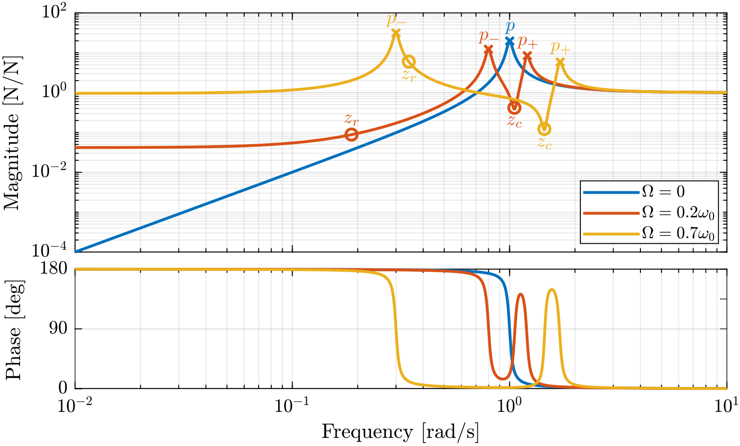

Fig.: Bode plot of the diagonal terms of $\boldsymbol{G}_f$ for several rotational speeds Ω

Decentralized IFF with Pure Integrators

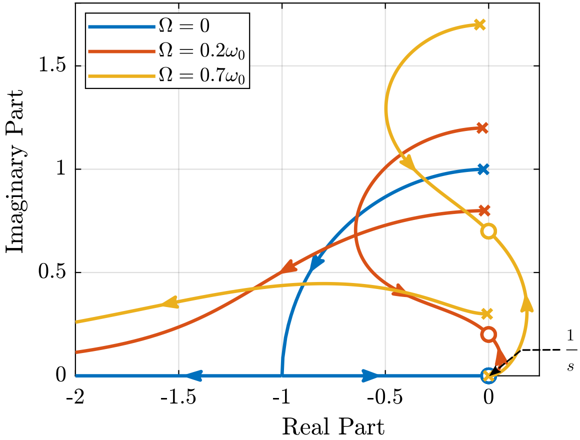

Fig.: Root Locus for Decentralized IFF for several rotating speeds Ω

For $\Omega > 0$, the closed loop system is unstable

Outline

Modification of the Control Low

$$K_F(s) = g \cdot \frac{1}{s} \cdot \underbrace{\frac{s/\omega_i}{1 + s/\omega_i}}_{\text{HPF}} = g \cdot \frac{1}{s + \omega_i}$$

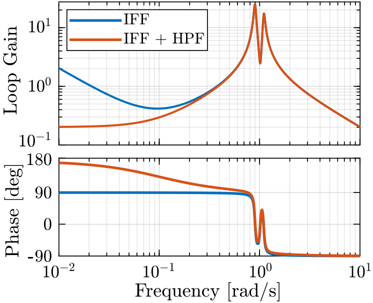

Fig.: Loop Gain

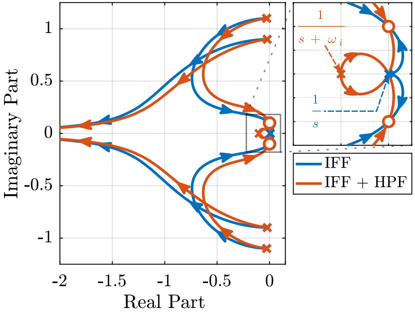

Fig.: Root Locus

Added HPF $\iff$ limit the low frequency gain

$\iff$ shift the pole to the left along the real axis

$\implies$ stable system for small values of the gain

Effect of ω_i on the attainable damping

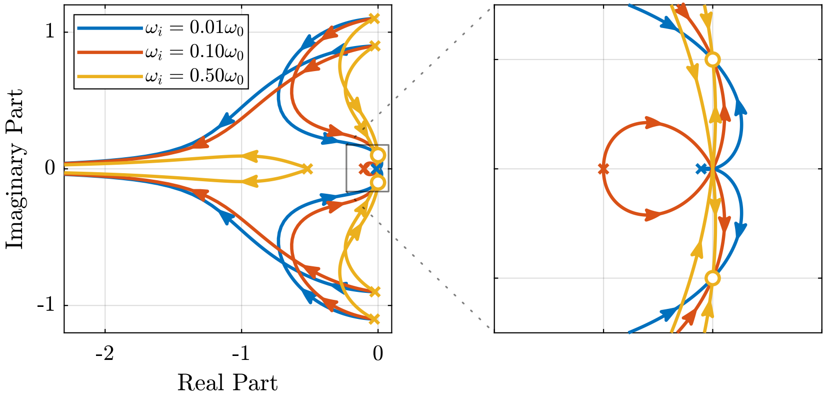

Fig.: Root Locus for several HPF cut-off frequencies ω_i, $\Omega = 0.1\omega_0$

$$g_{\mathsf{max}} = \omega_i \left(\frac{{\omega_0}^2}{\Omega^2} - 1 \right)$$

small $\omega_i \implies$ increase maximum damping
small $\omega_i \implies$ reduces maximum gain g_{max}

Optimal Control Parameters

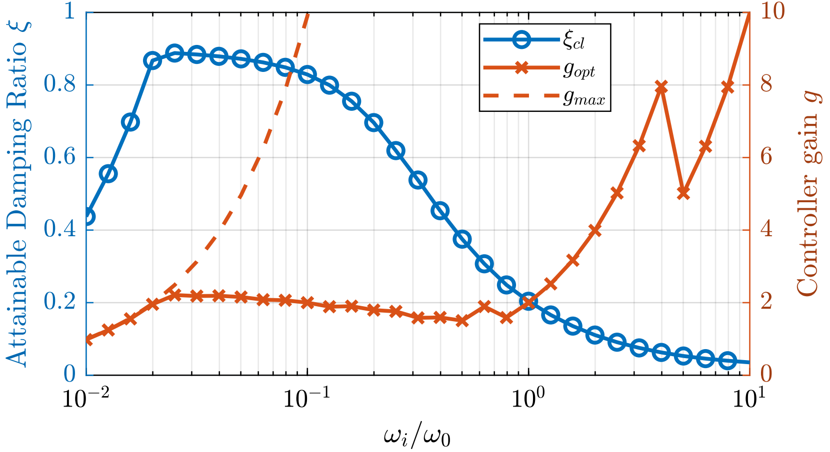

Fig.: Attainable damping ratio ξ_{cl} as a function of the ratio ω_i/ω_0. Corresponding control gain g_{opt} and g_{max} are also shown

Outline

Stiffness in Parallel with the Force Sensor

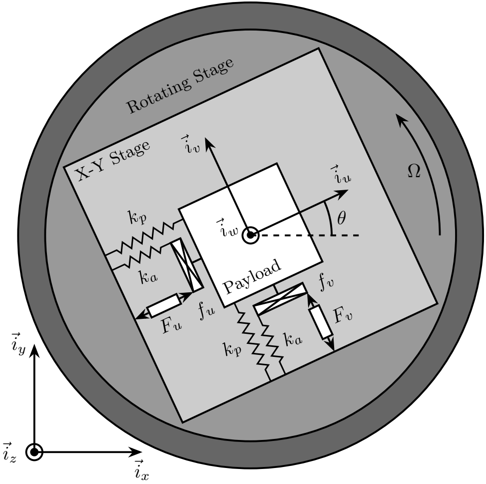

Fig.: Studied system with additional springs in parallel with the actuators and force sensors

Intuitive Idea

k_p is used to counteract the negative stiffness $-m\Omega^2$ when high control gains are used.

$$k_p = \alpha k$$
$$k_a = (1-\alpha)k$$

with $0 < \alpha < 1$.

The overall stiffness $k = k_a + k_p = \text{cst} \Longrightarrow$ the open-loop poles remains unchanged

Effect of the Parallel Stiffness on the Plant Dynamics

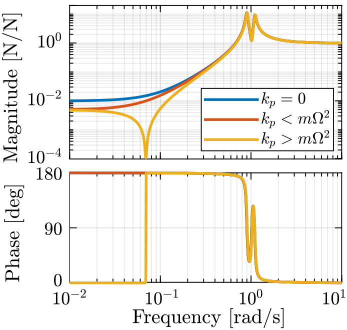

Fig.: Bode Plot of f_u/F_u for $k_p = 0$, $k_p < m\Omega^2$ and $k_p > m\Omega^2$, $\Omega = 0.1\omega_0$

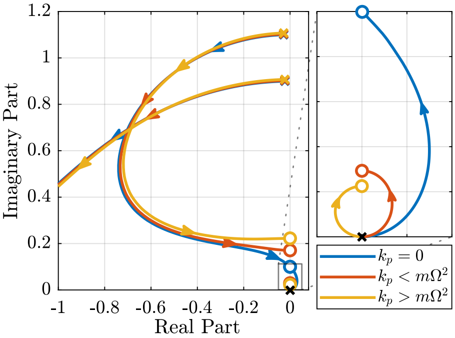

Fig.: Root Locus for IFF without parallel spring, with parallel springs with stiffness $k_p < m\Omega^2$ and $k_p > m\Omega^2$, $\Omega = 0.1\omega_0$

If $k_p > m\Omega^2$, the poles of the closed-loop system stay in the (stable) right half-plane, and hence the **unconditional stability of IFF is recovered**.

Optimal Parallel Stiffness

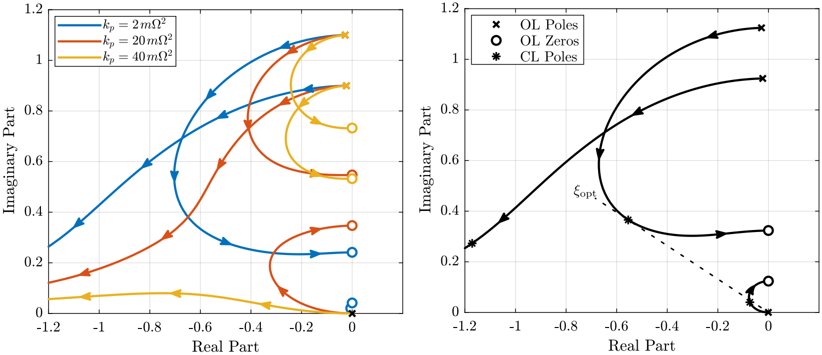

(a) Comparison of three parallel stiffnesses k_p

(b) $k_p = 5m\Omega^2$, optimal damping ξ_{opt} is shown

Fig.: Root Locus for IFF when parallel stiffness k_p is added, $\Omega = 0.1\omega_0$

Large parallel stiffness k_p reduces the attainable damping.

Outline

Comparison of the Attainable Damping

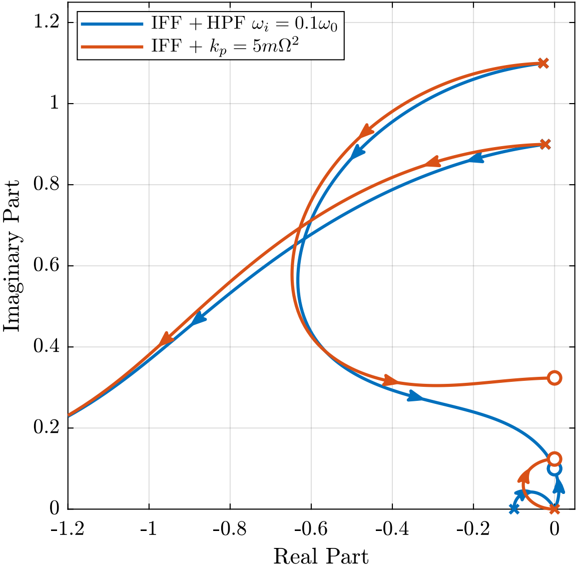

Fig.: Root Locus for the two proposed modifications of decentralized IFF, $\Omega = 0.1\omega_0$

Comparison Transmissibility and Compliance

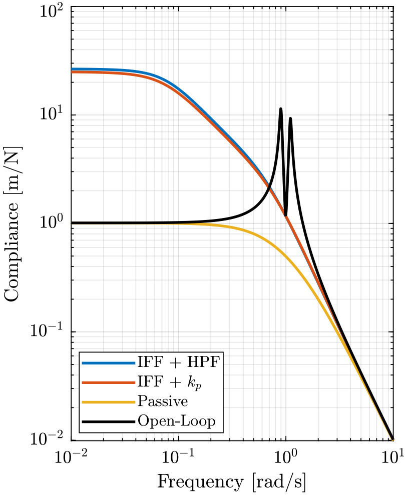

(a) Compliance

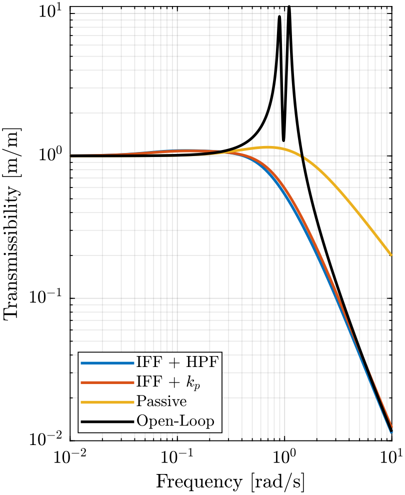

(b) Transmissibility

Fig.: Comparison of the two proposed Active Damping Techniques, $\Omega = 0.1\omega_0$

Conclusion & Further work

The two proposed techniques gives almost identical results but are very different when it comes to their implementations

The best technique depends on the application

Amplified Piezoelectric Actuators are a nice way to have an actuator, a force sensors and a parallel stiffness in a compact manner

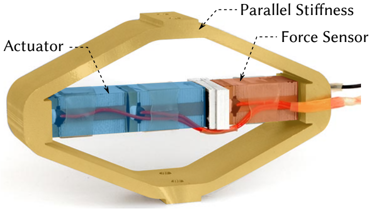

Will be tested on the nano-hexapod